SpaceOps Conferences
28 May - 1 June 2018, Marseille, France
2018 SpaceOps Conference

10.2514/6.2018-2566

Machine Learning Approach to Initial Orbit Determination of Unknown LEO Satellites

Byoung-Sun Lee[1] , Yoola Hwang[2], Dae-Won Kim[3]
Electronics and Telecommunications Research Institute (ETRI), Daejeon 34129, Republic of Korea

Won-Gil Kim[4]
Soletop, Daejeon 34051, Republic of Korea

and

Junho Lee[5]
Korea Aerospace Industry (KAI), Sacheon 52529, Republic of Korea

Downloaded by ISTRAC/ISRO Command Network on May 11, 2023 | http://arc.aiaa.org | DOI: 10.2514/6.2018-2566

Initial orbit determination should be performed to know the unknown satellite orbit with minimum observation data sets from ground station. Satellite tracking system such as optical, radar, and/or radio can acquire and track the satellite based on the initial orbit. Then a normal operational orbit determination is carried out with enough tracking data sets. However, initial acquisition and tracking of the unknown satellite are very difficult with conventional optical telescope, directional radar, and parabolic radio antenna system. When the unknown satellite transmits downlink radio signal, an omnidirectional radio antenna with wide-band receiving capability can acquire the Doppler signal from the satellite. A series of Doppler observations are converted to range rates between the satellite and ground station.

In this paper, only one real ground station is defined to measure range rate of the satellite and two virtual ground stations are assumed to predict range rate and slant range. Prediction of range rate and slant range is carried out by machine learning. One month of simulated tracking data set, i.e. range rate and slant range, for the three ground stations are used in the training. Given a satellite pass at the real ground station, predicted satellite tracking data from two virtual ground stations are generated by machine learning. Then, trilateration orbit determination is performed with range rate and slant range data sets from the three ground stations. This study shows that the regression of the machine learning is applicable to the initial orbit determination of the unknown satellites.

Nomenclature

GEO = Geostationary Earth Orbit
GS = Ground Station
IOD = Initial Orbit Determination
LEO = Low Earth Orbit
MAPE = Mean Absolute Percent Error
ML = Machine Learning
RAC = Radial, Along-track, and Cross-track
RF = Radio Frequency
SRMC = Satellite Radio Monitoring Center of Korea
TCA = Time of Closest Approach

[1] Managing Director/Principal Researcher, Unmanned Vehicle Systems Research Group, LBS@etri.re.kr.
Professor, Aerospace System Engineering Major, University of Science and Technology, LBS@ust.ac.kr.
[2] Principal Researcher, Unmanned Vehicle Systems Research Group, ylhwang@etri.re.kr.
[3] Senior Researcher, KSB Convergence Research Department, dwk@etri.re.kr.
[4] Junior Researcher, Development Division, wgkim@soletop.com.
[5] Engineer, KFX Flight Mechanics Team, junho.lee@koreaaero.com.

Copyright © 2018 by the American Institute of Aeronautics and Astronautics, Inc. All rights reserved.

Downloaded by ISTRAC/ISRO Command Network on May 11, 2023 | http://arc.aiaa.org | DOI: 10.2514/6.2018-2566

I. Introduction

Nowadays, Machine Learning (ML) is widely used in the engineering field to solve the classification and regression problems. In the satellite orbit determination and prediction area, a supervised ML has been applied to perform classification of RF transmissions and orbit determination of CubeSat[1], and improving the orbit prediction accuracy of resident space objects[2, 3]. Due to the efforts of many researchers in the past, satellite orbit dynamics have already been well known. Based on the satellite orbit dynamics theory and rely on the modern fast computer, a large amount of orbit-related data can be generated, trained in the ML, and used to solve some orbit-related problems caused by the measurement data insufficiency.

Tracking data in the Ground Station (GS) to determine the orbit of the satellite include azimuth, elevation (or right ascension and declination), slant range, and/or range rate. If a satellite orbit is not known it is very difficult to track the satellite with optical telescope, directional radar, and parabolic radio antenna system. However, when the satellite transmits a radio wave to the ground, it is possible to measure the Doppler shift of the satellite signal using an omnidirectional antenna capable of receiving the frequency. From this, a series of range rates between the satellite and GS can be obtained. If there are data sets of the slant range and the range rate simultaneously measured by three GSs for unknown satellites, initial orbit determination is possible using trilateration method.

In this paper, it is assumed that only one real GS equipped with omnidirectional antenna is available and only range rate data can be obtained in the GS. Two virtual GSs are defined to share the same satellite coverage as the real GS and locate apart enough for a good geometrical configuration. Initial orbit determination using trilateration method is carried out using measured range rate data in the real GS and the generated range rate and slant range data from two virtual GSs by ML. Slant range data in the real GS are also generated using range rate data by ML. A satellite in Sun-synchronous orbit with mean altitude of 550 km is assumed as unknown satellite. One month of simulated tracking data set including range rate and slant range for the three GSs are generated and trained in ML. Given a satellite pass at real GS, predicted satellite tracking data from two virtual GSs are generated by ML. Then the trilateration orbit determination is performed with range rate and slant range sets from the three GSs. The initial orbit of satellite is propagated to the next satellite pass and then check the possibility of reacquisition of the satellite with using conventional parabolic antenna. This study shows that the regression of the ML is applicable to the initial orbit determination of the unknown satellites.

II. Radio Tracking of the Satellite Signal

The methods to monitor and track the orbiting satellites can be broadly divided into radio, optical, radar and laser. Since there are advantages and disadvantages according to each method, it is necessary to operate all the methods together and complement each other in order to construct a national Space Situational Awareness (SSA) network. Radio tracking can track satellites regardless of night or day. However, it is possible to track only if the satellite is transmitting radio waves to the ground. When a parabolic antenna is used in a ground station, the antenna pointing direction must be known through satellite orbit prediction. The omnidirectional antenna can receive satellite radio waves without knowing the position of the satellite, but unlike a parabolic antenna, the antenna gain cannot be obtained.

Satellite Radio Monitoring Center (SRMC) of Korea[4] regularly tracks and monitors the satellite radio signal in Geostationary Earth Orbit (GEO) and Low Earth Orbit (LEO). There are two 13m Cassegrain antenna for GEO satellite, two full motion Cassegrain antenna and one parabolic antenna for LEO satellite. Three omnidirectional antenna with redundant configuration are installed to monitor radio waves of LEO satellites passing through the Korean Peninsula. The satellite radio monitoring frequency band is 137MHz-2GHz, 2-18GHz, and 18-26.5 GHz, which includes most of the satellite communications frequencies. An approximate satellite orbital period can be determined by monitoring the spectrum continuously for radio waves from LEO satellites. Measurement parameters include downlink frequency, bandwidth, Doppler shift, field strength, and polarization. However, LEO satellites usually pass over the ground station within about 15 minutes and wait for more than 1.5 hours until the next consecutive pass.

Figure 1 show the bird's eye view picture of SRMC. Four Cassegrain antenna and one parabolic antenna are shown in the picture. Figure 2 presents hemispherical cage for omnidirectional antenna system in SRMC. There are three kinds of omnidirectional antennas to cope with different frequencies from the satellites. Figure 3 shows the full motion parabolic antenna for the frequency band of 137MHz-2GHz.

Downloaded by ISTRAC/ISRO Command Network on May 11, 2023 | http://arc.aiaa.org | DOI: 10.2514/6.2018-2566



Fig. 1 Bird's eye view picture of SRMC, Korea. **Fig. 2 Omni antenna cage.** **Fig. 3 Parabolic antenna.**

Doppler shift can be used as satellite tracking data to determine the change of distance between the satellite and the GS. Satellite radio frequency received at the GS is increased relative to the actual transmission frequency as the satellite approaches to the GS and decreased as the satellite moves away. Doppler shift is zero at the Time of Closest Approach (TCA) of the satellite and the actual transmission frequency can be measured at the ground station. Satellite Doppler tracking system known as TRANET[5] was a network of radio receiving stations and other facilities operated by U.S. Navy from the year of 1963. In the DORIS (Doppler Orbitography and Radiopositioning Integrated by Satellite)[6] system, which is contrary to TRANET, LEO satellite measures Doppler shift by receiving the radio waves transmitting from ground station network. DORIS system is developed for precise orbit determination and precise ground location.

III. Generation of the Satellite Tracking Data for Machine Learning

In order to generate satellite tracking data for machine learning, we first calculated the Sun-synchronous orbital elements[7] for orbit propagation. Table 1 shows the sun-synchronous orbit with mean altitude of 550 km. Mean ascending node is calculated for ascending node passing time of 06:00 and initial mean eccentricity and mean argument of perigee are derived for making frozen orbit[8]. The osculating orbital elements are derived from mean orbital elements by iterative process. The osculating orbital elements are used for satellite orbit propagation and tracking data generation.

Table 1. Orbital Elements (Epoch: 2018-MAR-01 00:00:00 UTC)

	a (km)	e	i (deg)	Ω (deg)	ω (deg)	M (deg)
Mean	6928.137	0.001069	97.5930	248.7520	90.0000	0.0000
Osculating	6918.841	0.000701	97.5941	248.7538	269.0824	180.8855

As shown in Table 2, SRMC in Icheon City, Gyeonggi Province is used as GS for generating tracking data. Two virtual GSs, Jeju and Ulleung islands are designated taking into account the southern and eastern ends of the Korean peninsula.

Table 2. Locations of Three Ground Stations

	Latitude (deg)	Longitude (deg)	Height (km)
SRMC (real)	37.087	127.501	0.030
Jeju (virtual)	33.310	126.320	0.030
Ulleung (virtual)	37.290	130.540	0.030

The satellite tracking data was generated from March 1, 2018 for 30 days. The azimuth, elevation, range, and range rate data, which pass through SRMC, Jeju and Ulleung were obtained in respectively. By using the analytical orbit propagator[9] modeling only the J2 term was used for a large amount of data can be calculated in a short time while maintaining the characteristic of the sun synchronous orbit.

Figure 4 shows 152 ground traces passing through the SRMC, Jeju, and Ulleung. It can be seen that the ground traces are uniformly distributed in the entire contact area. There are both ascending passes and descending passes in the figure.

Figure 5 presents the elevation change of the satellite passing through the SRMC. As can be seen from Figure 4, there is an ascending path passing over the head of the SRMC, with a maximum elevation of 89.0 degrees, with a pass time of 735 seconds. Satellite azimuth vs. elevation information is shown in Figure 6 as a polar plot.

Figure 7 shows the range rate vs. elevation angle plot. Range rate starts with the maximum negative value at the satellite rising time, and reaches to zero at the time of closest approach, and ends with the maximum positive values at the satellite set time.

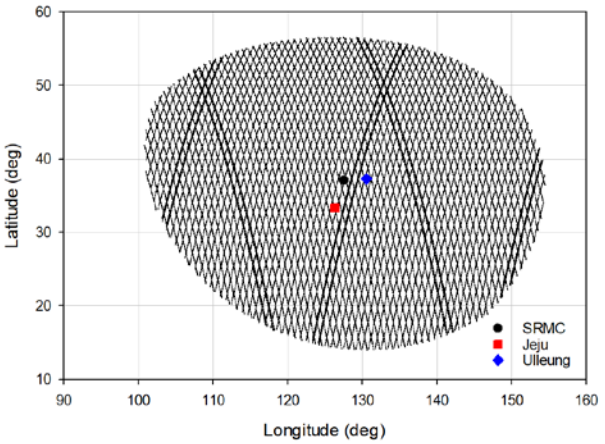

Fig. 4 Ground track of satellite pass.

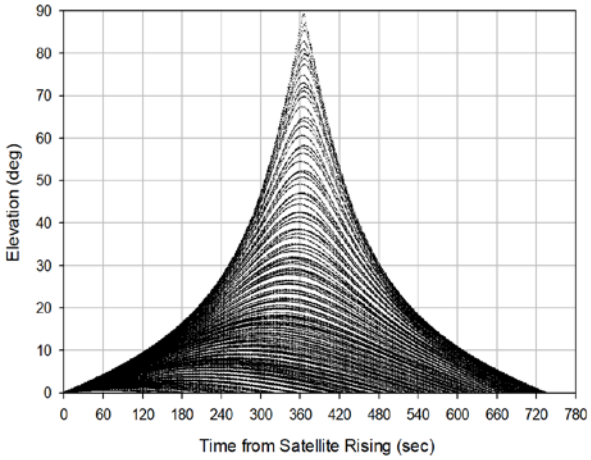

Fig. 5 Elevation angle of satellite pass.

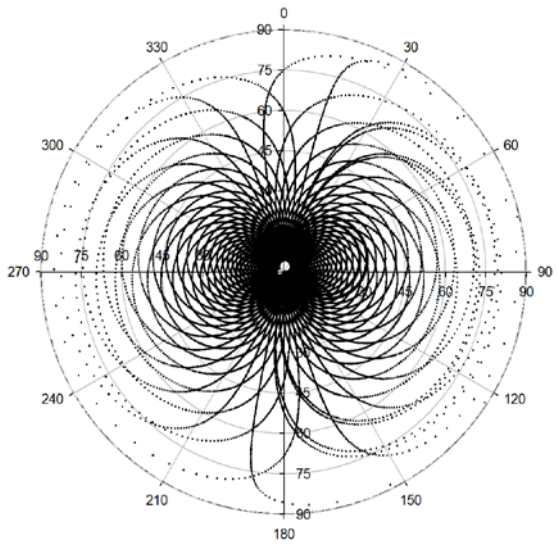

Fig. 6 Polar plot of satellite pass.

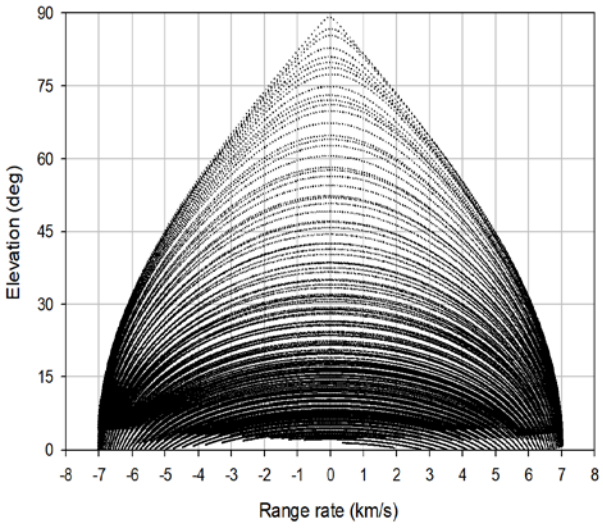

Fig. 7 Range rate vs. elevation.

Figure 8 presents variation of range rate with satellite passing time at GS. Range rate with zero means the satellite passes through closest point to the ground station. The change of range rate is the maximum at TCA. The maximum value of the range rate is calculated to be 7.0534 km/s. Totals of 73386 lines of tracking data at 1 second interval from 152 satellite passes over 30 days are generated and used for ML.

Downloaded by ISTRAC/ISRO Command Network on May 11, 2023 | http://arc.aiaa.org | DOI: 10.2514/6.2018-2566

Figure 9 shows variation of range with satellite passing time at GS. The maximum range is 2903.1 km and the minimum range is 556.2 km.

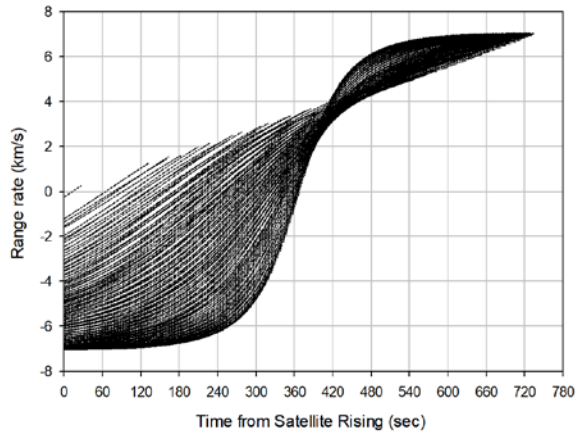

Fig. 8 Variation of range rate at SRMC.

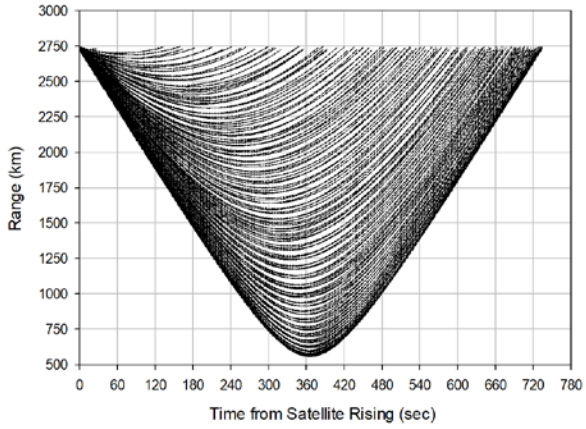

Fig. 9 Variation of range at SRMC.

Figure 10 presents the variation of elevations at the three GSs for the case of the maximum passing time at SRMC. At the time of maximum elevation at SRMC with 89.0 degrees, the elevation at Jeju is 49.2 degrees and the same at Ulleung is 62.5 degrees. The maximum elevation at Jeju is 87.3 degrees and the same at Ulleung is 63.8 degrees.

Figure 11 shows the variation of range rate at the three GSs for the case of the maximum passing time at SRMC. The TCAs at the three GSs are different one another. The time difference of TCA between Ulleung and SRMC is 11 seconds and the same between SRMC and Jeju is 61 seconds.

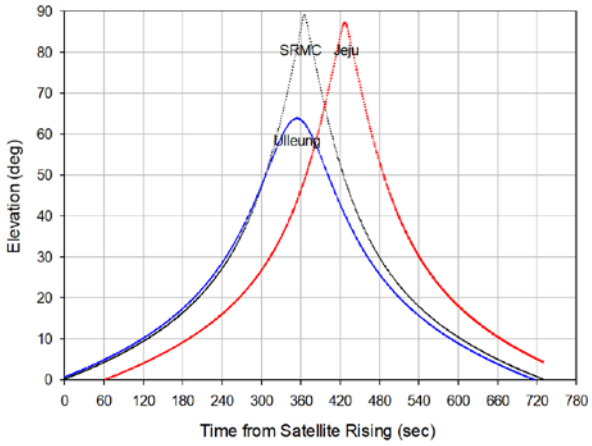

Fig. 10 Variation of range rate at three GSs.

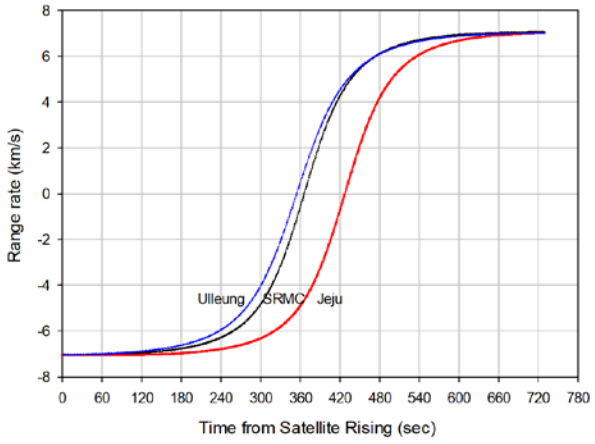

Fig. 11 Variation of range at three GSs.

IV. Machine Learning for Range Rate and Slant Range Data Generation

ML is used to generate range rate and slant range data at virtual stations in Jeju and Ulleung according to the time of the measured range rate data at SRMC. The slant range data at SRMC is also generated by ML. As explained in the previous section, one month of simulated tracking data, i.e. range rate and slant range data, for the three GSs are used in the training. Automated machine learning (AutoML) system called AUTO-SKLEARN[10] based on scikit-learn library is applied to train the satellite tracking data. AUTO-SKLEARN constructs an ensemble model consisting of several ML models, where each ML model is automatically selected and their hyperparameters are also automatically tuned by using Bayesian optimization and meta-learning methods. Scikit-learn is machine learning library[11] for the Python programming language.

Three features for machine learning of range rate are ground station contact time from satellite rising at SRMC, the range rate of three GSs, and the duration of the satellite pass at SRMC.

Downloaded by ISTRAC/ISRO Command Network on May 11, 2023 | http://arc.aiaa.org | DOI: 10.2514/6.2018-2566

Figure 12 shows three features in Machine Learning at SRMC. Range rates and durations of satellite passes at SRMC are presented based on the time from satellite rising at SRMC.

Figure 13 presents two different groups of range rate at Jeju based on the time from satellite rising at SRMC. It is because there are two different satellite passes such as ascending passes and descending passes.

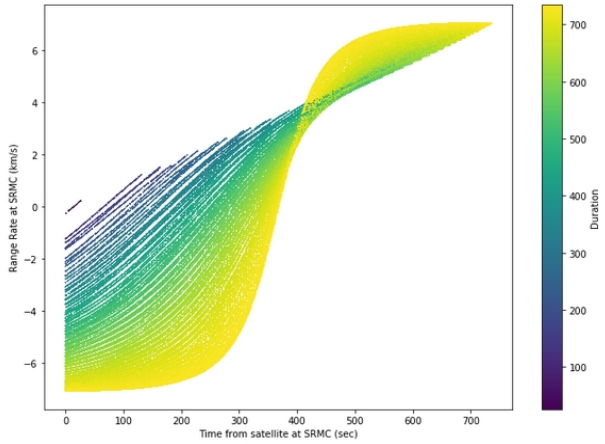

Fig. 12 Range rate at SRMC.

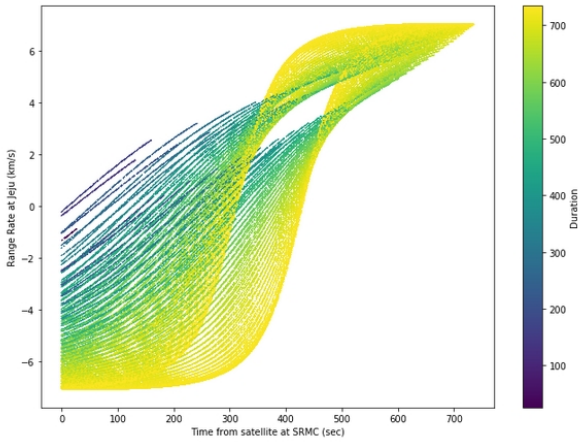

Fig. 13 Range rate at Jeju based on time at SRMC.

Figure 14 shows the ML training results of range rate at SRMC. Thirty days of satellite passes are used for training. True range rates at x-axis are input data and predicted range rate at y-axis are ML results. One diagonal straight line shows good training results. The Mean Absolute Percent Error (MAPE) in this case is 0.045527.

Figure 15 shows the ML results of range rate at Jeju, which does not take into account the ascending passes and the descending passes. The x-axis is featured range rate data and y-axis is predicted ML range rate output. The machine learning results are not good because the predicted range rates from ML are matched with many different values of input range rates. The MAPE in this case is 0.477229. To overcome this problem, total of 152 satellite passes are divided into two groups consisting of 71 ascending passes and 81 descending passes for machine learning input.

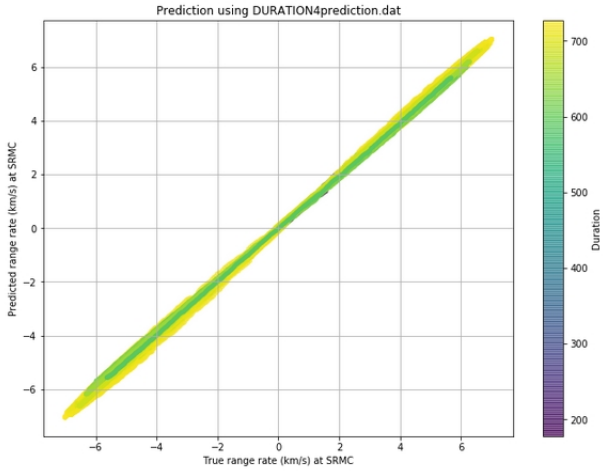

Fig. 14 Machine learning results at SRMC.

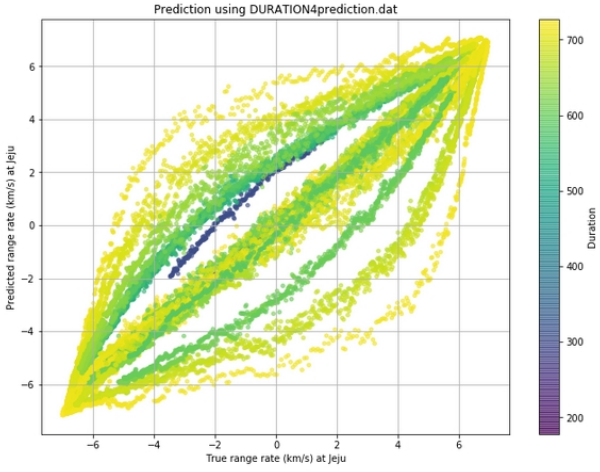

Fig. 15 Machine learning results at Jeju.

Figure 16 shows three features in ML for Jeju. The range rates and durations of satellite passes at Jeju are presented based on the time from satellite rising at SRMC. Two groups of range rate in Figure 13 are not shown in Figure 16 because only a total of 71 ascending passes are considered. Figure 17 presents the same features for Ulleung. A total of 71 ascending passes are considered here.

Downloaded by ISTRAC/ISRO Command Network on May 11, 2023 | http://arc.aiaa.org | DOI: 10.2514/6.2018-2566

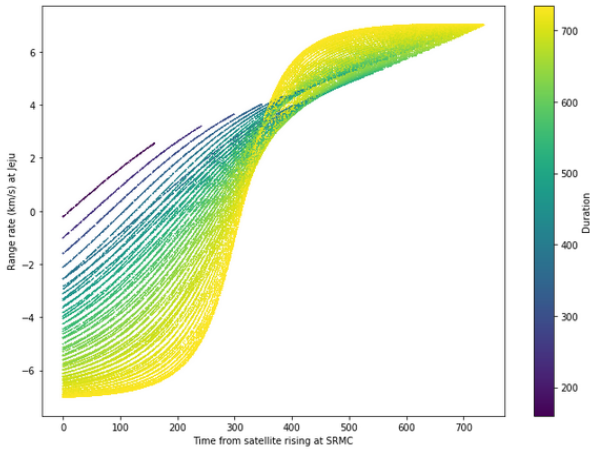

Fig. 16 Range rate to ML at Jeju.

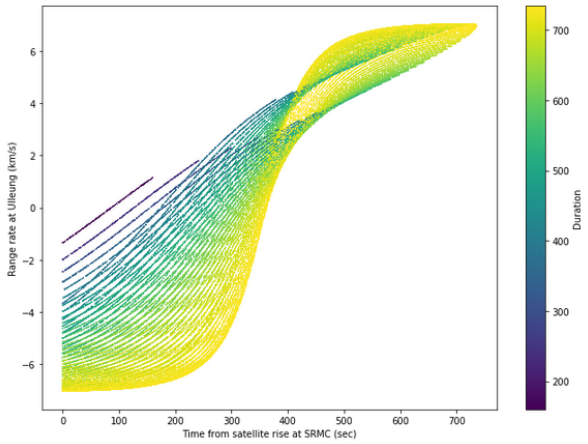

Fig. 17 Range rate to ML at Ulleung.

Based on ML training for one months of satellite ascending pass, a prediction of range rate for one satellite pass at two virtual GSs is performed. The time of satellite rising at SRMC is 20:16:13 UTC on April 1, 2018. And set time is 20:27:31 UTC on April 1, 2018. The duration of satellite pass at SRMC is 678 seconds. A total of 679 range rates in 1 second interval is predicted for Jeju and Ulleung by ML.

Figure 18 shows comparison of predicted range rate to true range rate at Jeju. In this case, true range rate is known because simulation data are used. Predicted range rates by ML are good and the MAPE is 0.0125279. Figure 19 presents the same comparison at Ulleung. The predicted range rate by ML at Ulleung is good and the MAPE is 0.0158166. The differences between the true and the predicted values will be presented later as in Figure 24. The predicted range rate data for two virtual GSs are used for IOD.

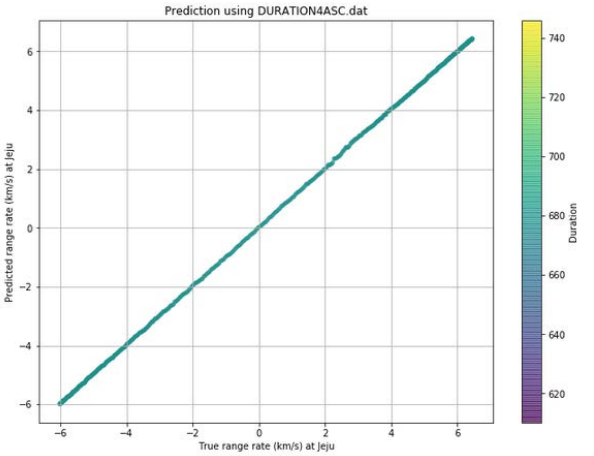

Fig. 18 Range rate at Jeju by ML.

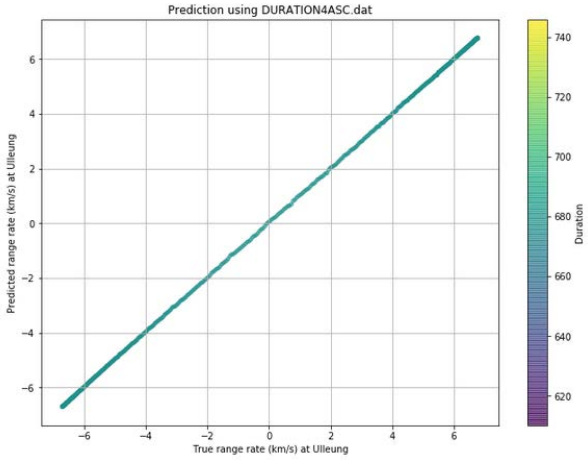

Fig. 19 Range rate at Ulleung by ML.

Slant range between the satellite and GS is not a measured value at SRMC because only Doppler shift can be measured using omnidirectional antenna. Machine learning is also used to generate slant ranges at SRMC based on the observed range rate data at SRMC. The features for ML of slant range at SRMC are GS contact time from satellite rising at SRMC, the range rate of GS at SRMC, and the duration of the satellite pass at SRMC. Figure 20 shows comparison of predicted range to true range at SRMC. Predicted ranges by ML are good and the MAPE is 0.006605.

In order to generate slant ranges at Jeju and Ulleung, slant ranges at SRMC for 30 days are added to the features to ML. Four features are GS contact time from satellite rising at SRMC, the range rates of GS at SRMC, and the duration of the satellite pass at SRMC. Figure 21 presents slant ranges to ML at SRMC.

Figure 22 and 23 present slant ranges to ML at Jeju and Ulleung. Predicted slant ranges by ML are good and the MAPE are 0.0041927 and 0.0035262 in respectively.

Downloaded by ISTRAC/ISRO Command Network on May 11, 2023 | http://arc.aiaa.org | DOI: 10.2514/6.2018-2566

Downloaded by ISTRAC/ISRO Command Network on May 11, 2023 | http://arc.aiaa.org | DOI: 10.2514/6.2018-2566

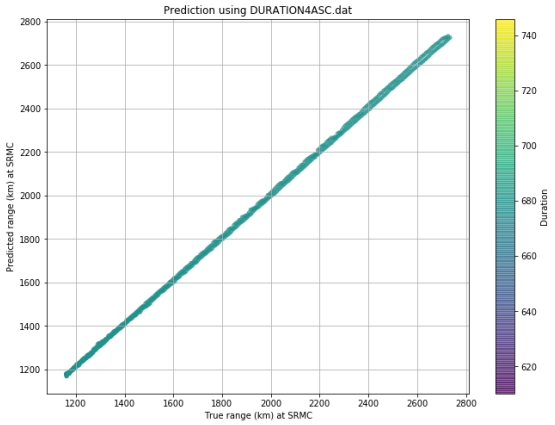

Fig. 20 Machine learning results at SRMC.

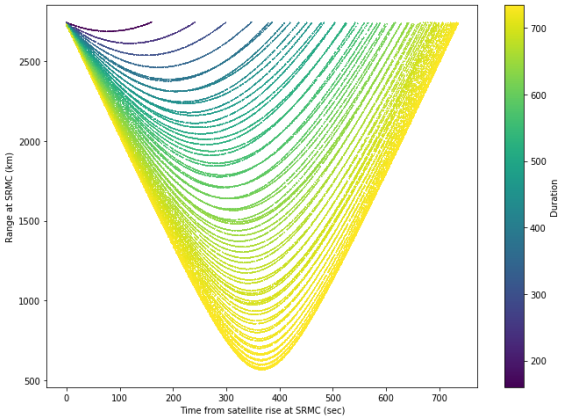

Fig. 21 Slant range to ML at SRMC.

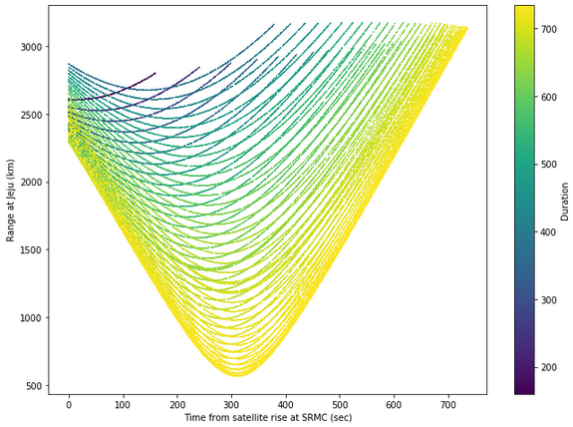

Fig. 22 Slant range to ML at Jeju.

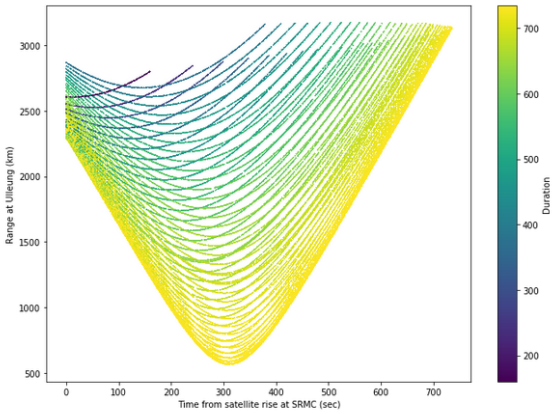

Fig. 23 Slant range to ML at Ulleung.

Figure 24 shows the difference between the true and predicted range rate by ML at Jeju and Ulleung. TCA is at 341 seconds from satellite rising at SRMC. The differences are bigger near TCA since the changes of range rate is higher near TCA. Figure 25 presents the slant range differences at Jeju, Ulleung, and SRMC. The differences are small at the satellite rising time and bigger near TCA. Generated slant range at SRMC is not good compared to Jeju and Ulleung because only range rate at SRMC is used as feature in ML.

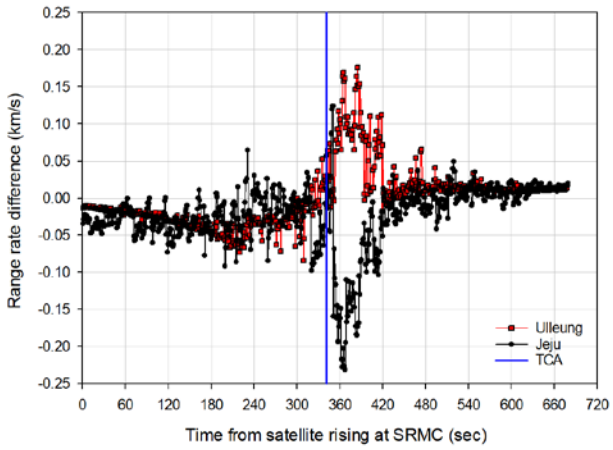

Fig. 24 Range rate difference.

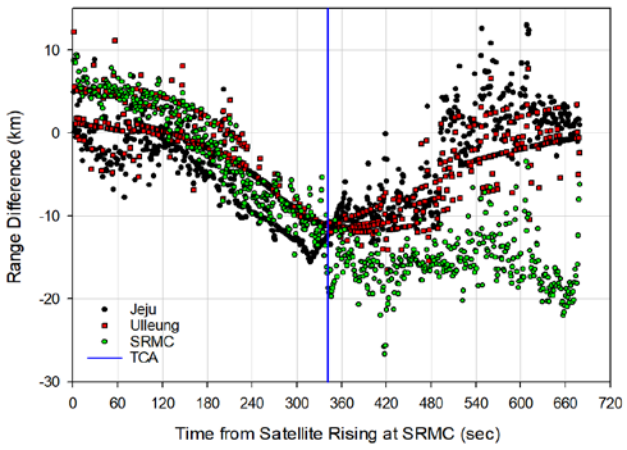

Fig. 25 Slant range difference.

V. Initial Orbit Determination Using Slant Range and Range Rate Data Set

Initial orbit determination of unknown satellite is carried out using three sets of slant range and range rate from three GSs. The exact solution by trilateration can be obtained because the simultaneous measurements from three GSs are available. Trilateration algorithm for the exact solution is well described in Escobal[12].

Figure 26 presents the trajectory of satellite passing through Korean peninsula. Figure 27 shows the geometrical configuration of trilateration. Three GSs are located in the Korean territory. The western part of the Earth is dark because the dawn-dusk Sun-synchronous orbit is applied.

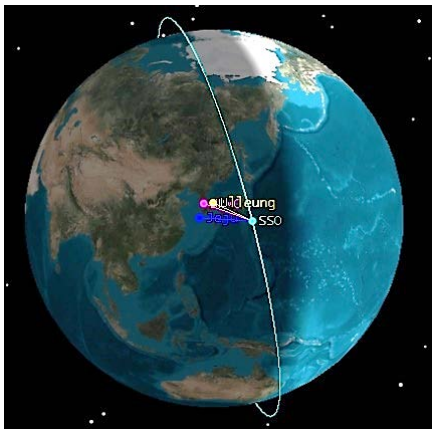

Fig. 26 Satellite trajectory.

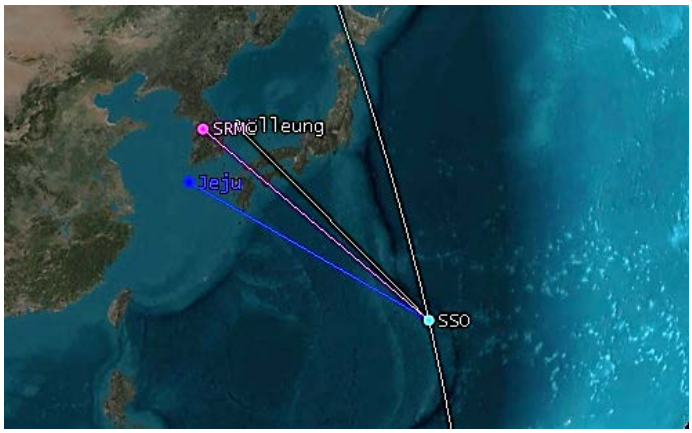

Fig. 27 Geometrical configuration of trilateration.

A series of trilateration orbit determinations are performed for the data sets from three GSs. Slant range and range rate data sets of 678 seconds from 20:16:13 UTC to 20:27:31 UTC on April 1, 2018 are used, and more than 600 of IOD results are obtained by trilateration.

Figure 28 shows the Radial, Along-track, and Cross-track (RAC) differences between the true orbit and IOD. Radial and along-track differences are bigger than cross-track ones. And the total position differences are relatively small near TCA.

Figure 29 presents ± 60 seconds of RAC differences centered by TCA. The total position differences are about 60 km. In order to check the possibility of reacquisition of the satellite next pass, IOD result at TCA is chosen to propagate the orbit. It is because a satellite radio transmission frequency can be obtained at TCA.

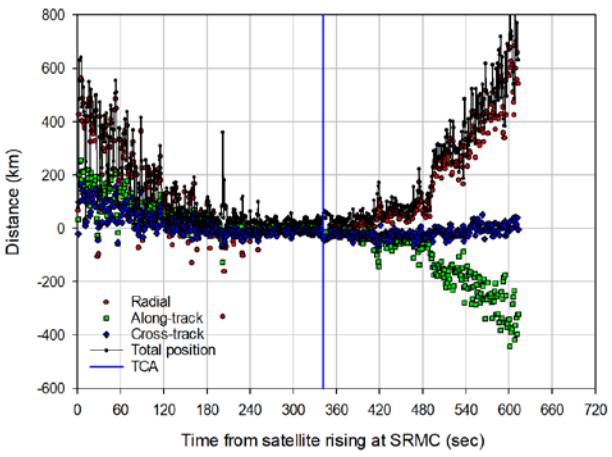

Figure 28. RAC differences.

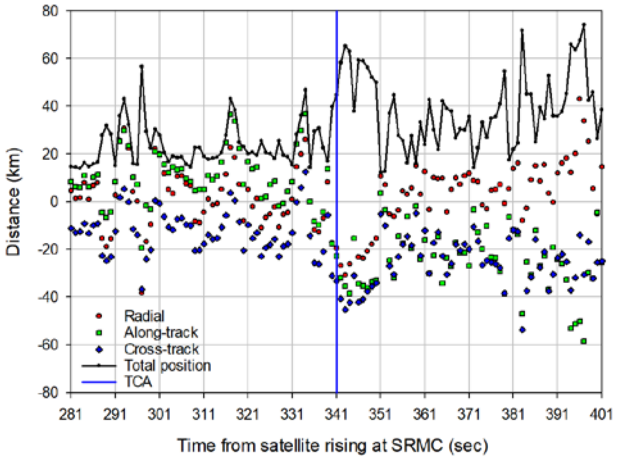

Figure 29. RAC differences near TCA.

Table 3 shows the satellite orbital elements at TCA. True orbit and IOD will be propagated to the next pass to check the possibility of tracking the satellite using parabolic antenna.

Downloaded by ISTRAC/ISRO Command Network on May 11, 2023 | http://arc.aiaa.org | DOI: 10.2514/6.2018-2566

Table 3. Orbital Elements (Epoch: 2018-APR-01 20:21:53 UTC)

	a (km)	e	i (deg)	Ω (deg)	ω (deg)	M (deg)
True	6929.8758	0.000701	97.5941	280.1021	160.8347	239.0218
IOD	6674.1317	0.077257	98.3024	281.0608	278.3223	113.6276

Figure 30 shows the azimuth and elevation plot of the next satellite pass which is propagated using true and IOD in Table 3. Table 4 presents satellite tracking parameters at rising time. There are 4 minutes differences in the satellite rising time. However, trends of the two trajectories are similar in Figure 30. Figure 31 presents zoomed-in trajectories of Figure 30 at the satellite rising. The azimuth differences between the true and IOD predictions are small enough to acquire the satellite signal using small parabolic antenna. The half-power-beam-width of the 5 m parabolic antenna for the reception of 2 GHz radio wave is estimated about 2.1 degrees.

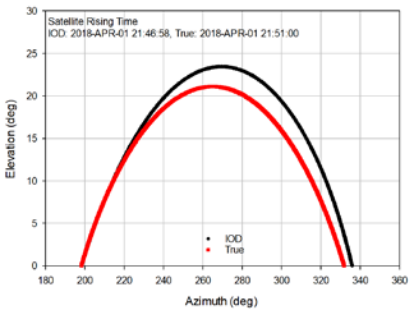

Fig. 30 Azimuth and elevation of the satellite pass.

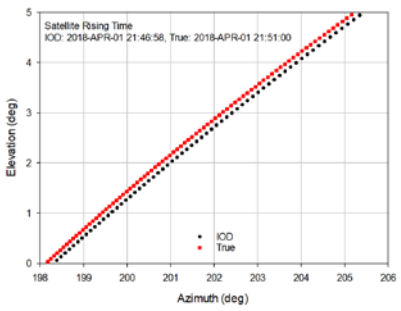

Fig. 31 Azimuth and elevation at satellite rising time.

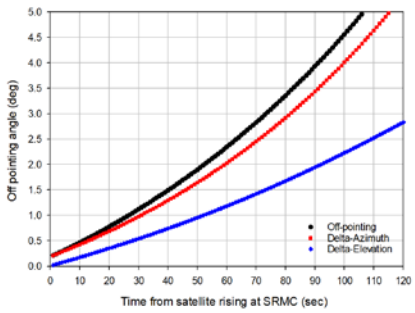

Fig. 32 Off-pointing angle at satellite rising time.

Table 4. Satellite Tracking Data at Rising Time

	Satellite Rising Time at SRMC	Azimuth(deg)	Elevation(deg)	Range(km)	Range rate(km/s)
True	2018-APR-1 21:51:00 UTC	198.1810	0.0340	2730.9700	-6.2961
IOD	2018-APR-1 21:46:58 UTC	198.3910	0.0590	2172.8550	-6.2706

Figure 32 shows the antenna off-pointing angle between the true and IOD predictions for 120 seconds from satellite rising. Less than 2 degrees of off-pointing angles are maintained for the first 50 seconds. In order to acquire the satellite radio signal and perform the mono-pulse tracking, parabolic antenna should be pointed to the satellite rising direction and waited until the satellite radio signal is coming. A sort of zigzag scanning of the mono-pulse antenna may be required to compensate the pointing errors. When the mono-pulse tracking antenna acquire the satellite radio signal, antenna pointing data such as time-tagged azimuth and elevation, and Doppler data can be obtained for the normal operational orbit determination.

VI. Concluding Remarks

IOD by trilateration method was carried out with the satellite measurement data from ML. One real GS and two virtual GSs were assumed to simulate and generate satellite measurement data. Range rate and slant range data from two virtual GSs corresponding to the range rate data at real GS were generated by ML. Slant range data from real GS also generated by ML based on the range rate data at real GS. One month of simulated measurement data for the three GSs were used in ML. IOD was performed using the measurement data for one satellite pass. The initial orbit at TCA time was propagated until the next satellite pass time, and then checked whether the satellite can be tracked using the conventional parabolic antenna. The difference in the rising direction of the satellite was so small enough to keep track of the satellite despite a delay of four minutes. It has been shown that ML can be applied to IOD of unknown satellites in the environment with limited measurement data and ground stations.

In this study, a one-month orbit data was applied to ML as a preliminary experiment. More research is needed to investigate how ML results improve when more data is used. When using only range rate data, it is required to find a way to distinguish the ascending pass or descending pass. Otherwise, two initial orbital elements can be created, which

Downloaded by ISTRAC/ISRO Command Network on May 11, 2023 | http://arc.aiaa.org | DOI: 10.2514/6.2018-2566

can lead to an undesirable situations where the antenna is pointing in a direction where the satellite does not come out. It is necessary to perform IOD using the actual Doppler data measured by an omnidirectional antenna in SRMC. Another problems are expected to arise when the real measurement data is used. Nonetheless, ML is also expected to be a very useful tool in the field of space situational awareness.

References

[1] Sharma, S. and J. W. Cutler, "Robust Orbit Determination and Classification: A Learning Theoretic Approach," JPL IPN PR 42-203, pp. 1-20, November 15, 2015.

[2] Peng, H. and Bai, X., “Limits of Machine Learning Approach on Improving Orbit Prediction Accuracy using Support Vector Machine”, Conference Proceedings of AMOS, Sep. 19-22, 2017.

[3] Peng, H. and Bai, X. “Improving orbit prediction accuracy through supervised machine learning”, Advances in Space Research, 2018 in press, https://doi.org/10.1016/j.asr.2018.03.001.

[4] Satellite Radio Monitoring Center, “Monitoring System”, URL: http://www.srmc.go.kr/en_srmc/en_main.do [cited 12 Apr. 2018].

[5] Dunnel, C. A., “TRANET Doppler Tracking System”, APL Technical Digest, March-April, 1967, pp. 17-23.

[6] International DORIS Service, “A Doppler satellite tracking system”, URL: https://ids-doris.org [cited 12 Apr. 2018].

[7] Chobotov, V. A. (ed.), Orbital Mechanics, AIAA, Reston, 1996, pp. 218-253.

[8] Lee, B.-S. and Lee, J.-S., “Selection of Initial Frozen Orbit Eccentricity and Evolution of the Orbit Due to Perturbations(in Korean)”, J. of KSAS, Vol. 25, No. 1, 1997, pp. 126-132.

[9] Markley, P.R. and Jeletic, J.F., "Fast Orbit Propagator for Graphical Display", J. of Guidance, Vol. 14, No. 2, 1991, pp. 473-475.

[10] Feurer, M., Klein, A., Eggensperger, K., Springenberg, J. T., Blum, M., and Hutter, F., “Efficient and Robust Machine Learning”, Proceedings of the 28th International Conference on Neural Information Processing Systems - Volume 2Pages 2755-2763, Montreal, Canada, December 07-12, 2015

[11] Pedregosa, F., Varoquaux, G., Gramfort, A., Michel, V., Thirion, B., Grisel, O., Blondel M., Prettenhofer, P., Weiss, R., Dubourg V., Vanderplas, J., Passos A., Cournapeau, D., Perrot M., and Duchesnay E., "Scikit-learn: Machine Learning in Python". Journal of Machine Learning Research. 12, 2011, pp. 2825-2830.

[12] Escobal, P. R, Methods of Orbit Determination R. E. Krieger, New York, 1976, pp. 309-312.

Downloaded by ISTRAC/ISRO Command Network on May 11, 2023 | http://arc.aiaa.org | DOI: 10.2514/6.2018-2566